J|A|C|S
ARTICLES
Published on Web 02/20/2007

Fingerprint Vibrational Spectra of Protonated Methyl Esters of Amino Acids in the Gas Phase

Aude Simon,*[,†,||] Luke MacAleese,[‡] Philippe Maître,[‡] Joël Lemaire,[‡,§] and Terrance B. McMahon[†]

Contribution from the Department of Chemistry, University of Waterloo, 200 University Avenue West, N2L3G1 Waterloo, Ontario, Canada, Laboratoire de Chimie-Physique d'Orsay, Faculté des sciences, UMR8000 CNRS-Université Paris Sud, Bâtiment 350, 91405 Orsay Cedex, France, and CLIO-LCP, Université Paris Sud, Bâtiment 209 D, 91405 Orsay Cedex, France

Received August 28, 2006; E-mail: aude.simon@cesr.fr

Abstract: Infrared spectra of the protonated monomers of glycine, alanine, valine, and leucine methyl esters are presented. These protonated species are generated in the gas phase *via* matrix assisted laser desorption ionization (MALDI) within the cell of a Fourier transform ion cyclotron resonance spectrometer (FTICR) where they are subsequently mass selected as the only species trapped in the FTICR cell. Alternatively, they have also been generated by electrospray ionization and transferred to a Paul ion-trap mass spectrometer where they are similarly isolated. In both cases IR spectra are then derived from the frequency dependence of the infrared multiple photon dissociation (IRMPD) in the mid-infrared region (1000−2200 cm^{-1}), using the free electron laser facility Centre de Laser Infrarouge d'Orsay (CLIO). IR bands are assigned by comparison with the calculated vibrational spectra of the lowest energy isomers using density functional theory (DFT) calculations. There is in general good agreement between experimental IRMPD spectra and calculated IR absorption spectra for the lowest energy conformer which provides evidence for conformational preferences. The two different approaches to ion generation and trapping yield IRMPD spectra that are in excellent agreement.

Introduction

Gas-phase experiments now allow isolated biologically active molecules to be characterized and fundamental biological processes[1] such as protein folding and enzyme substrate binding, to be probed.[2] In this context, both neutral[3−10] and ionic[2,11−18] biological species have been studied in the gas phase. With the use of soft ionization techniques, such as electrospray ionization (ESI)[19] and matrix assisted laser desorption ionization (MALDI),[20] large biological complexes, with masses ranging up to tens of kDa, can be transferred from either solution or solid state into the gas phase. A broad arsenal of mass spectrometric techniques can then be used to study these biological ions.[21] The recent development of mid-infrared spectroscopy of mass-selected ions using different ion traps is of particular interest since it offers the possibility of direct structural characterization of the ions. Gas-phase infrared spectra of small ionic systems such as protonated organic molecules first appeared more than two decades ago,[22−24] but these early spectra were limited to the 925−1090 cm^{-1} wavelength range of a CO_2 laser. Because of the low number density of ionic species in mass spectrometers, direct measurement of the infrared absorption is not possible, and, instead, "action spectroscopy" is employed to probe the consequences of infrared absorption. A common

† University of Waterloo.
‡ UMR8000 CNRS-Université Paris Sud.
§ CLIO-LCP, Université Paris Sud.
|| Current address: CESR, 9 avenue du Colonel Roche, 31028 Toulouse Cedex, France.

(1) Simons, J. P. *Phys. Chem. Chem. Phys.* **2004**, *6*, E7.
(2) Breuker, K. *Int. J. Mass Spectrom.* **2004**, *239*, 33.
(3) Chapo, C. N.; Paul, J. B.; Provencal, R. A.; Roth, K.; Saykally, R. J. *J. Am. Chem. Soc.* **1998**, *120*, 12956.
(4) Compagnon, I.; Oomens, J.; Bakker, J.; Meijer, G.; von Helden, G. *Phys. Chem. Chem. Phys.* **2005**, *7*, 13.
(5) Dian, B. C.; Clarkson, J. R.; Zwier, T. S. *Science* **2004**, *303*, 1169.
(6) Dian, B. C.; Longarte, A.; Zwier, T. S. *Science* **2002**, *296*, 2369.
(7) Florio, G. M.; Zwier, T. S. *J. Phys. Chem. A* **2003**, *107*, 974.
(8) Rizzo, T. R.; Park, Y. D.; Levy, D. H. *J. Chem. Phys.* **1986**, *85*, 6945.
(9) Robertson, E. G.; Simons, J. P. *Phys. Chem. Chem. Phys.* **2001**, *3*, 1.
(10) Snoek, L. C.; Kroemer, R. T.; Hockridge, M. R.; Simons, J. P. *Phys. Chem. Chem. Phys.* **2001**, *3*, 1819.
(11) Crowe, M. C.; Brodbelt, J. S. *J. Am. Soc. Mass Spectrom.* **2004**, *15*, 1581.
(12) Daneshfar, R.; Kitova, E. N.; Klassen, J. S. *J. Am. Chem. Soc.* **2004**, *126*, 4786.
(13) Fukui, K.; Naito, Y.; Akiyama, Y.; Takahashi, K. *Int. J. Mass Spectrom.* **2004**, *235*, 25.
(14) Jurchen, J. C.; Garcia, D. E.; Williams, E. R. *J. Am. Soc. Mass Spectrom.* **2003**, *14*, 1373.
(15) Jurchen, J. C.; Garcia, D. E.; Williams, E. R. *J. Am. Soc. Mass Spectrom.* **2004**, *15*, 1408.
(16) Meot-Ner, M. *J. Am. Chem. Soc.* **1974**, *96*, 3168.
(17) Meot-Ner, M. *The Ionic Hydrogen Bond in Complex Organics and Biomolecules*, 1st ed.; Elsevier: Oxford, U.K., San Diego, CA, 2003; Vol. 1, p 835.
(18) Price, W. D.; Schnier, P. D.; Williams, E. R. *J. Phys. Chem. B* **1997**, *101*, 664.
(19) Fenn, J. B.; Mann, M.; Meng, C. K.; Wong, S. F.; Whitehouse, C. M. *Science* **1989**, *246*, 64.
(20) Hillenkamp, F.; Karas, M.; Beavis, R.; Chait, B. *Anal. Chem.* **1991**, *63*, A1193.
(21) Williams, E. R.; Wysocki, V. H. *Int. J. Mass Spectrom.* **2002**, 219, VII.
(22) Peiris, D. M.; Cheeseman, M. A.; Ramanathan, R.; Eyler, J. R. *J. Phys. Chem.* **1993**, *97*, 7839.
(23) Thorne, L. R.; Beauchamp, J. L. *Infrared Photochemistry of Gas Phase Ions;* Academic Press: New York, 1984; Vol. 3, p 41.
(24) Woodin, R. L.; Bomse, D. S.; Beauchamp, J. L. *J. Am. Chem. Soc.* **1978**, *100*, 3248.

current technique is to monitor the photofragmentation yield of the mass-selected ion as a function of the IR laser frequency. Since the required energy for dissociating the ion is usually larger than the energy of a single infrared photon, the dissociation of interest usually requires the absorption of several photons. Thus, the action spectrum is the result of infrared multiple photon dissociation (IRMPD). Currently, IRMPD experiments employing a fixed frequency CO_2 laser are frequently used to sequence biopolymers together with other ion activation methods such as collision induced dissociation (CID) or electron capture dissociation (ECD).[25,26]

Free electron lasers (FEL), such as those at the Centre de Laser Infrarouge d'Orsay (CLIO) facility[27] in Orsay, France, and at the Free Electron Laser For Infrared Experiments (FELIX) facility[28] in Nieuwegein, Netherlands, provide excellent sources of high-intensity tunable infrared radiation that can be used to obtain spectra of mass-selected molecular ions in the mid-infrared region using this action spectrum approach.[29,30] In particular FTICR spectrometers have been employed at both CLIO[29,31] and FELIX[32−34] facilities to generate IR spectra of mass-selected biological ions.[35−40] It should also be noted that McLafferty and co-workers have shown[41] that IRMPD spectra can also be obtained using an OPO laser in the 3000−4000 cm^{-1} region which provides a valuable extension to the wavelength range accessible with the FEL facilities. However, the lower intensity of OPO lasers does not allow for as efficient an IRMPD process, particularly if the dissociation energy is too large, as in the case of some amino acid proton-bound dimers.[41]

Ionic species derived from amino acids have been the subject of extensive mass spectrometric investigations, and important gas phase thermochemical quantities, such as proton affinities and bond dissociation energies, have been determined.[16,18,42−48] A question of particular interest has been under what conditions gas-phase zwitterionic species might exist and attempts have been made to elucidate the factors influencing the stabilization of the zwitterionic form of amino acids.[3,49,50] Recently, IRMPD spectroscopy has been used to demonstrate that the complex of sodium ion, Na^+, with proline in the gas-phase exists predominantly in the zwitterionic form, whereas the complex of glycine with Na^+ exhibits a neutral, so-called charge solvated structure.[35] The coordination of the aromatic amino acid phenylalanine to the transition metal ions Ag^+ and Zn^{2+} has also been probed recently by IRMPD spectroscopy, and monocationic $[Ag^{I}\text{-Phe}]^+$ and deprotonated $[Zn^{II}\text{-Phe}_2\text{-H}]^+$ complexes have been studied.[40] The comparison with DFT calculations shows that a tridentate charge solvated structure is formed in the case of $[Ag\text{-Phe}]^+$, whereas a tetrahedral-type core structure is formed in the case of $[Zn\text{-Phe}_2\text{-H}]^{2+}$. The latter result is interesting as a mimic of the reactive centers in proteins since it is well-known that the coordination of Zn^{2+} in proteins is predominantly tetrahedral. IRMPD spectroscopy has also been shown to be valuable in determining the protonation sites of dipeptides,[37] and a very recent IRMPD spectroscopic study by McLafferty and co-workers on a large variety of proton-bound dimers of amino acids and polymers[51] has demonstrated the utility of IR spectroscopy for determining the characteristic spectral red-shifts associated with protonation of a variety of systems from amino acids to peptides in the 3050−3080 cm^{-1} range.

In the present work, IRMPD spectra are presented for the protonated methyl esters of glycine ($GlyMeH^+$), L-alanine ($AlaMeH^+$), L-valine ($ValMeH^+$), and L-leucine ($LeuMeH^+$) obtained at the CLIO FEL facility in the 1000−2200 cm^{-1}range. These spectra have been obtained using two different ionization techniques in two different mass spectrometers. In one case, a FTICR spectrometer was used for ion storage with MALDI generation of the species of interest and, in the other, a modified Paul-type ion-trap mass spectrometer was used with electrospray ion generation. The two experimental spectra are also compared to the IR absorption spectra of the lowest energy structures calculated at the density functional level of theory (DFT).[52] The comparison between experimental and theoretical results illustrates the power of the method to provide IR fingerprints of biologically relevant molecules in the gas phase and to distinguish between the different possible isomers. In particular, evidence is provided for intramolecular $C{=}O\cdots H^+$ interactions within the protonated monomers. The methods developed in this work constitute a step in our ongoing effort for the elucidation of infrared signatures to provide insight into the

(25) Sleno, L.; Volmer, D. A. *J. Mass Spectrom.* **2004**, *39*, 1091.
(26) Zubarev, R. A. *Mass Spectrom. Rev.* **2003**, *22*, 57.
(27) Prazeres, R.; Glotin, F.; Insa, C.; Jaroszynski, D.; Ortega, J. M. *Eur. Phys. J. D* **1998**, *3*, 87.
(28) Oepts, D.; van der Meer, A. F. G.; Amersfoot, P. W. *Infrared Phys. Technol.* **1995**, *36*, 297.
(29) Lemaire, J.; Boissel, P.; Heninger, M.; Bellec, G.; Mestdagh, H.; Simon, A.; Le Caer, S.; Ortega, J. M.; Glotin, F.; Maitre, P. *Phys. Rev. Lett.* **2002**, *89*, 273002/1.
(30) Oomens, J.; Sartakov, B. G.; Tielens, A.; Meijer, G.; von Helden, G. *Ap. J.* **2001**, *560*, L99.
(31) Maître, P.; LeCaer, S.; Simon, A.; Jones, W.; Lemaire, J.; Mestdagh, H.; Heninger, M.; Mauclaire, G.; Boissel, P.; Prazeres, R.; Glotin, F.; Ortega, J. M. *Nucl. Instr. Methods. A* **2003**, *507*, 541.
(32) Moore, D. T.; Oomens, J.; Eyler, J. R.; Meijer, G.; von Helden, G.; Ridge, D. P. *J. Am. Chem. Soc.* **2004**, *126*, 14726.
(33) Oomens, J.; Moore, D. T.; von Helden, G.; Meijer, G.; Dunbar, R. C. *J. Am. Chem. Soc.* **2004**, *126*, 724.
(34) Valle, J. J.; Eyler, J. R.; Oomens, J.; Moore, D. T.; van der Meer, A. F. G.; von Helden, G.; Meijer, G.; Hendrickson, C. L.; Marshall, A. G.; Blakney, G. T. *Rev. Sc. Inst.* **2005**, 76.
(35) Kapota, C.; Lemaire, J.; Maître, P.; Ohanessian, G. *J. Am. Chem. Soc.* **2004**, *126*, 1836.
(36) Lucas, B.; Gregoire, G.; Lemaire, J.; Maitre, P.; Glotin, F.; Schermann, J. P.; Desfrancois, C. *Int. J. Mass Spectrom.* **2005**, *243*, 105.
(37) Lucas, B.; Grégoire, G.; Lemaire, J.; Maître, P.; Ortega, J. M.; Rupenyan, A.; Reimann, B.; Schermann, J. P.; Desfrançois, C. *Phys. Chem. Chem. Phys.* **2004**, *6*, 2659.
(38) Polfer, N. C.; Paizs, B.; Snoek, L. C.; Compagnon, I.; Suhai, S.; Meijer, G.; von Helden, G.; Oomens, J. *J. Am. Chem. Soc.* **2005**, *127*, 8571.
(39) Oomens, J.; Polfer, N.; Moore, D. T.; van der Meer, L.; Marshall, A. G.; Eyler, J. R.; Meijer, G.; von Helden, G. *Phys. Chem. Chem. Phys.* **2005**, *7*, 1345.
(40) Polfer, N. C.; Oomens, J.; Moore, D. T.; von Helden, G.; Meijer, G.; Dunbar, R. C. *J. Am. Chem. Soc.* **2006**, *128*, 517.
(41) Oh, H.-B.; Breuker, K.; Sze, S. K.; Ge, Y.; Carpenter, B. K.; McLafferty, F. W. In Secondary and tertiary structures of gaseous protein ions characterized by electron capture dissociation mass spectrometry and photofragmentation spectroscopy. *Proc. Natl. Acad. Sci. U.S.A.* **2002,** p 15863.
(42) Kish, M. M.; Wesdemiotis, C.; Ohanessian, G. *J. Phys. Chem. B* **2004**, *108*, 3086.
(43) Locke, M. J.; Hunter, R. L.; McIver, R. T. *J. Am. Chem. Soc.* **1979**, *101*, 272.
(44) McLuckey, S. A.; Cameron, D.; Cooks, R. G. *J. Am. Chem. Soc.* **1981**, *103*, 1313.
(45) Meot-Ner, M. *J. Am. Chem. Soc.* **1984**, *106*, 278.
(46) Meot-Ner, M.; Hunter, E. P.; Field, F. H. *J. Am. Chem. Soc. 101.* **1979**, *3*, 686.
(47) Raspopov, S. A.; McMahon, T. B. *J. Mass Spectrom.* **2005**, *40*, 1536.
(48) Simon, A.; McMahon, T. B. *Int. Mass J. Spectrom. 301*, 255−256.
(49) Julian, R. R.; Hodyss, R.; Beauchamp, J. L. *J. Am. Chem. Soc.* **2001**, *123*, 3577.
(50) Price, W. D.; Jockusch, R. A.; Williams, E. R. *J. Am. Chem. Soc.* **1997**, *119*, 11988.
(51) Oh, H.-B.; C., L.; Hwang, H. Y.; Zhai, H.; Breuker, K.; Zabrouskov, V.; Carpenter, B. K.; McLafferty, F. W. *J. Am. Chem. Soc.* **2005**, *127*, 4076.
(52) Stevens, P. J.; Devlin, F. J.; Chablowski, C. F.; Frisch, M. J. *J. Phys. Chem. A* **1994**, *98*, 11623.

conformation of ions derived from small amino acids and other biologically relevant molecules in the gas phase.

Experimental Methods

Two different mass spectrometric techniques employing two different ionization methods were used to carry out the present work. The first of these was based on a home-built portable FTICR instrument, MICRA (for mobile ICR analyzer), described in detail previously,[53] using MALDI ionization, and the second involved a Bruker Esquire3000+ Paul-type ion-trap instrument suitably modified to provide optical access for the FEL beam. The CLIO FEL facility[27] is based on emission from a 10−50 MeV electron beam. Once the electron energy is fixed, the photon energy can be tuned by adjusting the gap of the undulator which is placed in the optical cavity. In the present work, the electron energy was set to either 42 MeV or 45 MeV to continuously scan the photon energy in the 950−1850 or 1200−2400 cm^{-1} energy ranges, respectively. The IR-FEL output consists of macropulses 8 μs in length with a repetition rate of 25 Hz. Each macropulse consists of approximately 500 micropulses, each of a few picoseconds duration. For a typical average IR power of 500 mW, the corresponding micropulse and macropulse energies are 40 μJ and 20 mJ, respectively. The mean IR power was stable and about 700−800 mW when recording the IRMPD spectrum with the Paul trap in the 800−1900 cm^{-1} energy range. It was slightly lower and about ∼400 mW when recording the IRMPD spectrum with the FTICR in the 1200−2400 cm^{-1} energy range. The laser wavelength profile was monitored while recording the spectra using a monochromator whose output led to a pyroelectric detector array (spiricon). The IR-FEL spectral width can be adjusted through a tuning of the optical cavity length, and the laser spectral width (fwhm) was typically less than 0.5% of the central wavelength. For both mass spectrometers, the same 1 m focal length spherical mirror was used to mildly focus the IR-FEL beam at the center of the ion trap, and its position was then fine-tuned so as to maximize the fragmentation efficiency.

The experimental spectra in the 1200−2400 cm^{-1} energy range were recorded using the portable FTICR, MICRA. This experimental configuration has been described in detail previously.[29,31,54] MICRA is based on a 1.24 T permanent magnet with the magnetic field perpendicular to the bore of the magnet which has two important consequences for the experiment. First, the IR beam enters perpendicular to the magnetic field and, owing to ion motion in the electric field along the magnetic field axis, this may result in a time dependent overlap of the IR beam with the ion cloud. Second, this arrangement does not allow for the use of external ion generation which restricts ionization to either in-cell or near-cell methods. Use of MALDI ion generation in this apparatus has been described previously.[35−37] Briefly, a sample MALDI target is made from a solid solution of the hydrochloride salt of the amino acid ester of interest mixed with α-cyano-4-hydroxycinamic acid (CHCA) in a 1:1 mass ratio which is then compressed into a 1 mm thick pellet. A 4 × 4 mm piece of this pellet was glued on a metallic holder which was then mounted just outside the ICR cell, ∼6 mm away from the middle of the nearest trapping plate. Desorption and ionization were then performed using the third harmonic (355 nm) of a pulsed Nd:YAG laser. The cations formed by MALDI enter the ICR cell collinearly with the magnetic field through a 5 mm diameter aperture. The ion signal was optimized by applying a 3.5 V potential to the trapping plate, while maintaining the target holder at a static potential of 1.8 V. The voltage of the entrance trapping plate was pulsed down to 0 V for 25 μs just after the laser pulse in order to optimize the ion transfer into the cell and then back to 3.5 V for trapping.

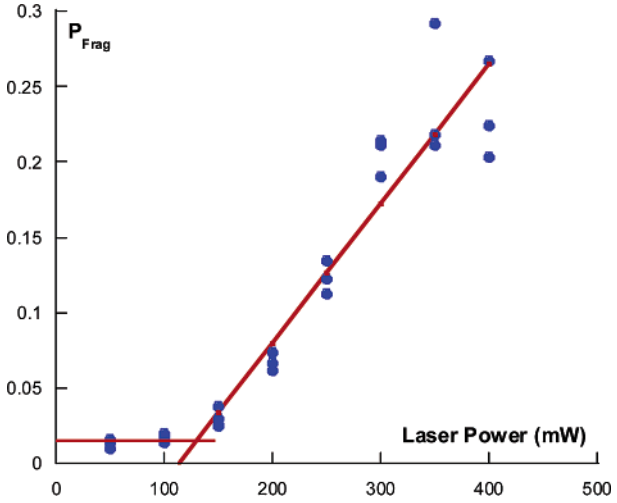

Figure 1. IRMPD efficiency as a function of laser power recorded at 1732 cm^{-1} for the protonated monomer of L-leucine methylester ($LeuMeH^+$).

The protonated amino acid ester ions thus generated were mass selected 100 ms after the Nd:YAG pulse, allowed to relax for 100 ms through collisions with a background inert gas, and subsequently irradiated with the IR beam for 1s (i.e., 25 IR-FEL macropulses). Detection was effected 50 ms after the end of the irradiation period. This duty cycle, ending with a quench pulse, was repeated eight times for each photon energy used and the mass spectrum obtained was the Fourier transform of the accumulated time domain signal.

The experimental spectra in the 950−1900 cm^{-1} energy range were recorded using a modified Bruker Esquire 3000 Paul ion-trap mass spectrometer. This experimental configuration has been described in detail previously.[54] The protonated amino acid ester ions were sprayed from a 10^{-5} M solution of the hydrochloride salts of the esters in water. A conical hole was drilled in the ring electrode of the Paul ion trap in order to allow optical access to the center of the trap. The IR-FEL beam enters through a ZnSe window oriented near the Brewster angle to allow the maximum transmission. Multistage mass spectrometry was carried out using the standard Bruker Esquire software. Within the MS1 step, a single isotope was mass-selected in a window of 1 Da for the ions of interest. The control of the irradiation time of the ions was performed using the MS2 step where the excitation amplitude was set to zero, and the associated output trigger was used to control the optical shutter, which was then opened for a fixed number of the IR-FEL macropulses. In most cases, mass selected ions were irradiated with a single IR-FEL macropulse. Mass spectra were recorded after accumulation of ten such sequences, and replicate spectra were acquired seven times for each photon energy, which was increased in steps of ∼4 to 5 cm^{-1}.

The IRMPD spectra reported here are expressed as the fragmentation efficiency P_{frag} defined by eq 1, as a function of the photon energy, in cm^{-1}.

$$P_{frag} = -\ln(I_{parent}/(I_{parent} + \Sigma I_{fragment})) \quad (1)$$

In each of the four cases examined, a single ionic photofragment was observed, the $(R)CH{=}NH_2^+$ immonium ion where R = H, CH_3, *i*-propyl, or i-butyl, corresponding to the loss of CO and CH_3OH.

Equation 1 assumes that the dissociation through IRMPD is a first-order process. As has been reported for other systems presenting large IR absorption cross-sections,[29] saturation could occur in the FTICR experiments when the laser was in resonance with the most strongly active IR modes. Conversely, when the IRMPD spectra were recorded with a laser beam attenuated by a factor of 3, no significant IRMPD signal was detectable associated with the weak IR absorption bands, with intensity less than 40 km mol^{-1}. This nonlinear behavior is illustrated in Figure 1 for protonated leucine methyl ester where the

(53) Mauclaire, G.; Lemaire, J.; Boissel, P.; Bellec, G.; Heninger, M. *Eur. J. Mass Spectrom.* **2004**, *10*, 155.
(54) Mac Aleese, L.; Simon, A.; McMahon, T. B.; Ortega, J.-M.; Scuderi, D.; Lemaire, J.; Maître, P. *Int. Mass J. Spectrom.* 2006, *14*, 249−250.

IRMPD efficiency has been monitored as a function of the laser power, when the IR-FEL was in resonance with the CO stretch (1732 cm^{-1}). As can be seen from Figure 1, the IRMPD efficiency scales linearly with the laser power from 130 through 400 mW, but a laser power threshold is observed at ~130 mW in this case. Since the laser power threshold strongly depends on the infrared absorption cross-section, no fluence correction has been applied to the fragmentation efficiency and only the raw IRMPD spectra, with intensities as defined by eq 1, are provided and compared to the calculated absorption spectra.

Computational Methods. The potential energy surfaces of each of the protonated amino acid esters were explored at the B3LYP/6-31+G-(d,p) level of theory using the Gaussian 98 package.[55] In each case, vibrational spectra of the two lowest energy isomers were then calculated within the harmonic approximation. With the use of appropriate scaling factors, hybrid DFT methods such as B3LYP have been shown to be capable of outperforming other DFT methods as well as traditional *ab initio* post-Hartree−Fock approaches in describing both the positions[56] and relative intensities[57] of IR bands. This is particularly true if instead of a uniform scaling factor, dual scaling factors are used,[56] one for the X−H stretching modes and the other, closer to 1, for the vibrational modes below 1800 cm^{-1}. A scaling factor of 0.98, previously shown to be optimal for metal cation complexes of amino acids[35] as well as protonated methyl esters of amino acids,[54] in this wavelength range, has been applied to all calculated frequencies reported in the present work. It must be also noted that, in the case of induced fragmentations such as those examined here, the absorption of the first photons may be followed by multiple absorption within a quasi-continuum wherein vibrational transitions may be slightly red-shifted and broadened owing to anharmonic couplings.[35] This possible effect will be discussed below in conjunction with comparison of the FTICR and Paul-trap spectra.

Results

1. Overview. The IRMPD spectra observed for the protonated amino acid esters in the present work can be usefully divided into three spectral regions for purposes of discussion. These regions are (i) the region from 800 to 1100 cm^{-1}, which was examined only using the Paul trap with electrospray ionization, and which can be mainly attributed to coupled rocking, bending, and deformation modes of the CH_3, NH_3, and CH_2 groups; (ii) two or more relatively intense and well structured bands in the 1200−1500 cm^{-1} corresponding to umbrella or deformation modes of the methoxy CH_3 and NH_3 groups; and (iii) a strong feature near 1750 cm^{-1} associated with the carbonyl stretching vibration.

Extensive searches of possible energetically favorable conformers on the potential energy surfaces of various protonated amino acids have been performed recently,[50,58−67] and in the lowest energy structures the proton is found to be bound to the most basic site in the molecule, the amino group. The corresponding structures for the analogous esters species have also been found to be the lowest energy structures in each of the four cases examined. In the ground-state structure, a further stabilizing interaction results from an intramolecular hydrogen bond between a hydrogen of this protonated amino group and the carbonyl oxygen of the carboxylate ester group. A second structure, slightly higher in energy, has also been located in each case in which one of the hydrogens of the protonated amino group also interacts instead with the methoxy oxygen of the carboxylate ester functionality. These two structures exhibit sufficiently different vibrational features that they should, in principle, be distinguishable from the experimental IRMPD spectra and, as will be seen below, this indeed appears to be the case.

2. Assignment of the IRMPD Spectrum of GlyMeH$^+$. The IRMPD spectra of GlyMeH$^+$ recorded in the FTICR and the Paul ion traps are reported in Figure 2, spectra a and b, respectively, together with the IR absorption spectra of the two lowest energy structures **MGly1** and **MGly2** (Figure 2c,d). For both of these structures protonation occurs on the most basic site, the amino group, which is also hydrogen bonded to either carbonyl oxygen of the carboxylate ester group (**MGly1**) or to the methoxy oxygen of the ester function (**MGly2**). In agreement with the extensive structural studies of protonated amino acids derivatives,[50,58−67] the structure corresponding to the ammonium group interacting with the carbonyl, **MGly1**, was found to be the most stable. In the present case, the structure **MGly2** was found to be 5.4 kcal mol^{-1} higher in energy.

As can be seen readily in Figure 2, there is a good agreement between the two observed IRMPD spectra of GlyMeH$^+$ generated within two different experimental conditions, either by MALDI and trapped into the ICR cell (Figure 2a) or by ESI and trapped into a Paul ion-trap (Figure 2b). Significantly, each of the four strongest bands observed is slightly red-shifted in the FTICR spectra relative to those observed in the Paul ion-trap spectra, by an average of 20 cm^{-1}. As discussed below, it is probable that the IRMPD spectra recorded under FTICR conditions are more prone to being red-shifted as compared to the calculated IR absorption spectra than are the corresponding IRMPD spectra obtained with the Paul trap. We will see that this effect is less pronounced in the case of protonated esters of amino acids presenting a larger alkyl chain than glycine. Nevertheless, the comparison of the two IRMPD spectra of each protonated ester of amino acid reveals that the IRMPD spectrum recorded using the Paul trap systematically presents the best resolution. In the present case of GlyMeH$^+$, the bandwidth (fwhm) is typically 40−45 cm^{-1} in the FTICR infrared spectrum (Figure 2a), and 25−30 cm^{-1} in the corresponding Paul ion-trap spectrum (Figure 2b). While the positions of the IRMPD bands are tabulated, we will essentially discuss the IRMPD spectrum obtained using the Paul trap and compare it to the corresponding calculated IR absorption spectra.

There is a good agreement between the observed IRMPD spectra of GlyMeH$^+$ and the calculated IR spectrum of the most stable conformer, **MGly1,** having the intramolecular hydrogen-bond interaction with the carbonyl oxygen (Figure 2c). The two calculated structures have markedly different carbonyl stretching frequencies, with **MGly2** exhibiting a strong absorption at 1823

(55) Frisch, M. J.; et al. *Gaussian 98*, revision A.6; Gaussian, Inc.: Pittsburgh, PA, 1998.
(56) Halls, M. D.; Velkovski, J.; Schlegel, H. B. *Theor. Chem. Acc.* **2001**, *105*, 413.
(57) Halls, M. D.; Schlegel, H. B. *J. Chem. Phys.* **1998**, *109*, 10587.
(58) Hoyau, S.; Pelicier, J. P.; Rogalewicz, F.; Hoppilliard, Y.; Ohanessian, G. *Eur. J. Mass Spectrom.* **2001**, *7*, 303.
(59) Jockusch, R. A.; Lemoff, A. S.; Williams, E. R. *J. Phys. Chem. A* **2001**, *105*, 10929.
(60) Jockusch, R. A.; Lemoff, A. S.; Williams, E. R. *J. Am. Chem. Soc.* **2001**, *123*, 12255.
(61) Komaromi, I.; Somogyi, A.; Wysocki, V. H. *Int. J. Mass Spectrom.* **2005**, *241*, 315.
(62) Moision, R. M.; Armentrout, P. B. *J. Phys. Chem. A* **2002**, *2002*, 10350.
(63) Rodgers, M. T.; Armentrout, P. B. *J. Am. Chem. Soc.* **2002**, *124*, 2678.
(64) Rogalewicz, F.; Hoppiliard, Y. *Int. J. Mass Spectrom.* **2000**, *199*, 235.
(65) Rogalewicz, F.; Hoppilliard, Y.; Ohanessian, G. *Int. J. Mass Spectrom.* **2000**, *196*, 565.
(66) Rogalewicz, F.; Hoppilliard, Y.; Ohanessian, G. *Int. J. Mass Spectrom.* **2003**, *227*, 439.
(67) Talley, J. M.; Cerda, B. A.; Ohanessian, G.; Wesdemiotis, C. *Chem.−Eur. J.* **2002**, *8*, 1377.

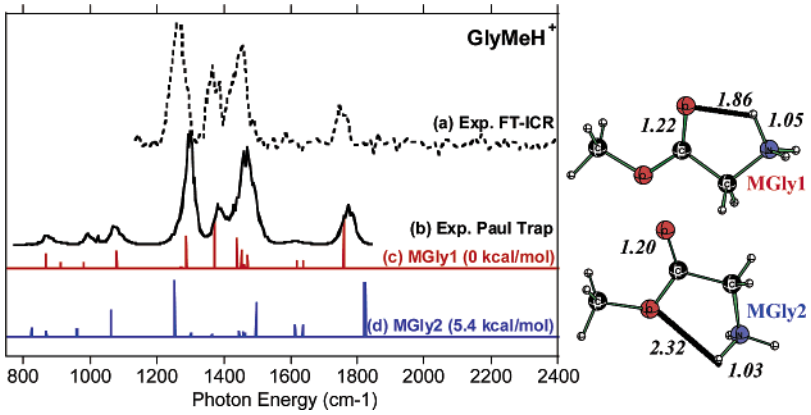

Figure 2. IR spectra of protonated glycine methyl ester $GlyMeH^+$. Experimental IRMPD spectrum recorded using 25 IR-FEL macropulses with the FTICR (a) and only one IR-FEL macropulse with the Paul ion trap (b) compared to the DFT calculated IR absorption spectra of the lowest energy conformer MGly1 (c) and a higher energy conformer MGly2 (d). The optimized structures of the two lowest energy conformers MGly1 and MGly2 are represented beside the spectra. The indicated distances are expressed in Å

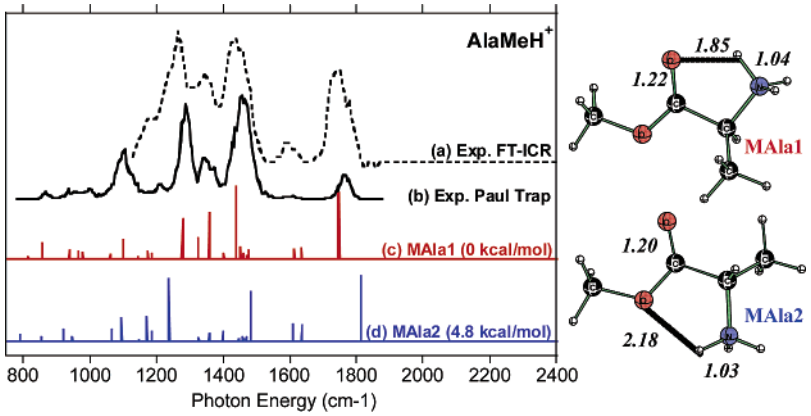

Figure 3. IR spectra of protonated alanine methyl ester $AlaMeH^+$. Experimental IRMPD spectrum recorded using 25 IR-FEL macropulses with the FTICR (a) and only one IR-FEL macropulse with the Paul ion trap (b) compared to the DFT calculated IR absorption spectra of the lowest energy conformer MAla1 (c) and a higher energy conformer MAla2 (d). The optimized structures of the two lowest energy conformers MAla1 and MAla2 are represented beside the spectra. The indicated distances are expressed in Å.

cm^{-1} which is less red-shifted than in **MGly1** (1758 cm^{-1}), in which the carbonyl strongly interacts with the protonated amino group. In the IRMPD spectrum obtained using the Paul trap, this band occurs at 1771 cm^{-1}, in good agreement with the value calculated for **MGly1**. The significant IRMPD intensity observed at 1471 cm^{-1} in the Paul trap can be assigned to the NH_3^+ umbrella motion. This vibration is calculated to occur at 1439 cm^{-1} in **MGly1** and at 1498 cm^{-1} in **MGly2**. Thus this -NH_3^+ umbrella motion is also found to be quite sensitive to its environment, and since the two different conformations represent quite different hydrogen bond environments for the ammonium group this mode can again be taken to be diagnostic of the presence of **MGly1** in these experiments. There is also a good match between the positions of the IRMPD bands observed and those calculated for the other two strong bands in the 1100−1500 cm^{-1} range. Experimentally, two maxima are observed at 1297 and 1386 cm^{-1} in the Paul trap. For the strongly absorbing bands calculated to occur in this region of the spectrum, only **MGly1** exhibits a vibration in the 1350−1400 cm^{-1} range, at 1372 cm^{-1} thus close to the experimental value at 1386 cm^{-1}. Furthermore, the observed band at 1297 cm^{-1} agrees well with the calculated 1287 cm^{-1} value for **MGly1**. The calculated IR spectrum of **MGly2** exhibits a strong IR mode (1254 cm^{-1}) in this region but significantly lower in energy than the observed band at 1297 cm^{-1}. Therefore, results in this spectral range also support the virtually exclusive presence of **MGly1** under our experimental conditions.

The IRMPD spectrum in the 800−1200 cm^{-1} energy range was only recorded for $GlyMeH^+$ formed by electrospray in the Paul ion trap (Figure 2b). Three bands were observed at 871, 992, and 1070 cm^{-1}. The positions as well as the relative intensities of these bands nicely match with the ones of the calculated spectrum of the most stable isomer **MGly1** (868, 981, and 1081 cm^{-1}), and the average difference is 8 cm^{-1} in the case of **MGly1**. The calculated IR spectrum of **MGly2** also displays IR active vibration in the 800−1200 cm^{-1} energy range, and this isomer presents in particular a vibrational transition at 825 cm^{-1} while no IRMPD signal was observed below 868 cm^{-1}. It thus seems that the 800−1200 cm^{-1} region provides an additional proof that the most stable isomer **MGly1** is the only isomer present in the Paul ion trap.

3. Assignment of the IRMPD Spectrum of $AlaMeH^+$. The IRMPD spectra of $AlaMeH^+$ recorded using the FTICR and the Paul ion trap are reported in Figure 3, spectra a and b. Once again, there is good agreement between the two sets of experimental data. However, the observed FTICR absorptions for the six most intense vibrations are consistently red-shifted relative to the Paul ion-trap data, again by an average of 16 cm^{-1}. As in the case of $GlyMeH^+$, it is also noteworthy that the $AlaMeH^+$ Paul ion-trap data exhibit a better resolution. The

calculated IR absorption spectra of the two lowest energy structures of $AlaMeH^+$ are given in Figure 3c,d as **MAla1** and **MAla2**. As was found for $GlyMeH^+$, in both **MAla1** and **MAla2**, protonation occurs on the amino group which is either coordinated to the carbonyl oxygen (**MAla1**) or to the methoxy oxygen of the carboxylate ester function (**MAla2**). As in the case of $GlyMeH^+$, the former structure was found to be the more stable, with the latter lying 4.8 kcal mol^{-1} higher in energy.

As in the case of protonated glycine methyl ester there are several key features in the spectra of **MAla1** and **MAla2** that permit them to be distinguished, and the experimental spectra clearly fit better with the spectrum calculated for the lower energy **MAla1** isomer. The most prominent difference between the spectra of **MAla1** and **MAla2** is once again associated with the IR signature of the stretching mode of the carbonyl group in the high-energy region of the IR spectrum. In **MAla1**, the vibrational frequency associated with the carbonyl group stretch of 1748 cm^{-1} is significantly lower in energy (66 cm^{-1}) as compared to the position at 1814 cm^{-1} in **MAla2** where the intramolecular hydrogen bond is weaker. The maximum in the Paul ion-trap IRMPD spectrum in this region was observed at 1764 cm^{-1}, only 16 cm^{-1} to the blue of the calculated position for the C═O stretch in **MAla1**. Since no IRMPD signal was observed above 1800 cm^{-1} using either method and considering that the C═O stretch is calculated to have a very high integrated IR absorption intensity, this would strongly suggest that **MAla1** is the only species formed in significant amount under the present conditions.

A second band significantly affected by the hydrogen-bonding environment is the strongly IR active band attributed to the umbrella mode of the protonated amino group. This mode is calculated to be located at 1438 cm^{-1} in **MAla1** which matches well with the intense IRMPD feature observed at 1456 cm^{-1} while less so with that calculated for **MAla2** which is located at 1482 cm^{-1}. A further argument against the presence of **MAla2** is the fact that a significant IRMPD signal is observed near 1350 cm^{-1}, whereas the **MAla2** species is not calculated to have a significant IR cross-section in this region. In contrast, **MAla1** is predicted to display a significant IR absorption intensity at 1357 cm^{-1}. It is also significant that the calculated **MAla1** spectrum predicts two absorptions in this region at 1325 and 1357 cm^{-1}, and the experimental spectrum does indeed reveal a bimodal structure to the feature observed.

The remaining five features observed in the IRMPD spectrum have thus been assigned on the basis of a good correspondence presumed with the calculated IR absorption frequencies for **MAla1**. The weakest band observed in the IRMPD spectrum is located near 1600 cm^{-1} and disappears completely when the laser power is decreased to 100 mW in the FTICR spectrum. The calculations attribute this band to the resonance of two moderately IR active modes, but the near-degeneracy (1612 and 1636 cm^{-1} in **MAla1**) of the asymmetric deformation modes of NH_3^+ is likely to be favorable for the multiple photon absorption process. The intense peak observed at 1286 cm^{-1} corresponds well to that predicted to occur at 1279 cm^{-1} and can be attributed to a combination of C−H bending, CH_3, and NH_3^+ rocking and C−O stretching modes. Another weak, but well resolved, feature in the Paul trap spectrum at 1220 cm^{-1} is also predicted by calculations to occur at 1188 cm^{-1} and corresponds to a combination of CH_3 and NH_3^+ rocking motions.

Three bands are observed in the 800−1150 cm^{-1} energy range using the Paul ion trap. Unfortunately, the calculated IR absorption spectra of the **MAla1** and **MAla2** species are very similar in this energy range. For instance, the IRMPD band at 1104 cm^{-1} can be assigned as ammonium and methyl group rocking motions coupled to a CCH wagging motion, calculated to occur at 1103 and 1097 cm^{-1} for **MAla1** and **MAla2**, respectively. Similarly, the peak observed at 868 cm^{-1} can be assigned as a rocking mode of the ammonium and the two methyl groups with simultaneous O−C−O and C_α−H bending modes based on the calculated frequency of such a normal mode for **MAla1** (859 cm^{-1}) and **MAla2** (855 cm^{-1}).

The conclusion that the experimental IRMPD spectrum corresponds essentially exclusively to **MAla1**, the lowest energy isomer of $AlaMeH^+$, would suggest that, even though a potentially energetic mode of ion formation such as MALDI would permit access to the higher energy conformer, apparently sufficient relaxation can occur within the time scale of the experiment that all such species which might be formed have rearranged to the energetic minimum. In addition to the very good agreement between the experimental and calculated positions of the bands in the IRMPD spectrum of $AlaMeH^+$ and the calculated spectrum of **MAla1**, it should be noted as well that there is a very good correspondence between the predicted and observed relative intensities.

4. Assignment of the IRMPD Spectrum of $ValMeH^+$. The IRMPD spectrum of $ValMeH^+$ recorded using the FTICR and Paul ion trap are reported in Figure 4, spectra a and b, respectively. In this case, the positions of the band maxima in the two spectra are in excellent agreement with, once again, the Paul ion-trap spectra exhibiting somewhat better resolution. The two lowest energy structures **MVal1** and **MVal2** of the protonated monomer $ValMeH^+$ are also given in Figure 4, spectra c and d, respectively, along with the corresponding IR absorption spectra. **MVal1** is the lowest energy isomer with **MVal2** lying 4.1 kcal mol^{-1} higher in energy.

As in the cases of $GlyMeH^+$ and $AlaMeH^+$, there is a good agreement between the experimental IRMPD spectrum and the calculated IR absorption spectrum of the most stable conformer **MVal1** (Figure 4c). As in the previous cases, the 1700−1850 cm^{-1} region clearly favors the assignment of the species present as **MVal1** since the carbonyl stretch, calculated to occur at 1745 cm^{-1} is in excellent agreement with the observed bands at 1747 cm^{-1} in the FTICR and 1749 cm^{-1} in the Paul ion trap. In contrast, the weaker intramolecular hydrogen bond present in **MVal2** structure is calculated to exhibit a carbonyl stretch at 1809 cm^{-1} and no IRMPD signal was observed above 1780 cm^{-1}.

A broad but structured absorption feature was observed in the 1200−1500 cm^{-1} range. In both experimental spectra, four maxima were located at 1247, 1284, 1334, and 1435 cm^{-1} in the Paul ion-trap infrared spectrum. Of these, a second IR structural diagnostic can be found in the NH_3^+ umbrella mode, which is predicted to occur at 1438 cm^{-1} in **MVal1** and at 1493 cm^{-1} in **MVal2** where the intramolecular hydrogen bond between an ammonium ion and the methoxy oxygen is weaker than that in **MVal1**. The position of the maximum in this

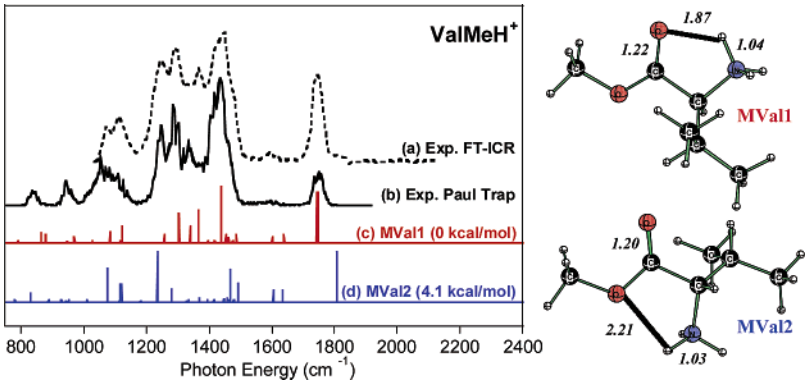

Figure 4. IR spectra of protonated valine methyl ester ValMeH$^+$. Experimental IRMPD spectrum recorded using 25 IR-FEL macropulses with the FTICR (a) and only one IR-FEL macropulse with the Paul ion-trap (b) compared to the DFT calculated IR absorption spectra of the lowest energy conformer MVal1 (c) and a higher energy conformer MVal2 (d). The optimized structures of the two lowest energy conformers MVal1 and MVal2 are represented beside the spectra. The indicated distances are expressed in Å.

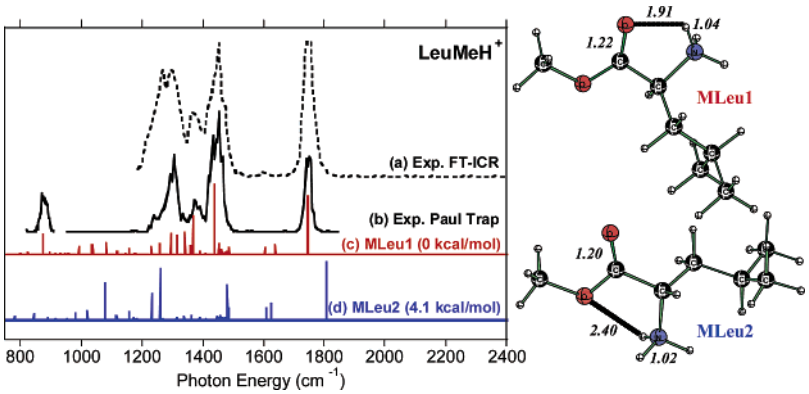

Figure 5. IR spectra of protonated leucine methyl ester LeuMeH$^+$. Experimental IRMPD spectrum recorded using 25 IR-FEL macropulses with the FTICR (a) and only one IR-FEL macropulse with the Paul ion trap (b) compared to the DFT calculated IR absorption spectra of the lowest energy conformer MLeu1 (c) and a higher energy conformer MLeu2 (d). The optimized structures of the two lowest energy conformers MLeu1 and MLeu2 are represented beside the spectra. The indicated distances are expressed in Å.

structured band observed in the IRMPD spectrum (1434 cm^{-1} with the ion trap) is in excellent agreement with the position (1438 cm^{-1}) in the calculated **MVal1** IR spectrum. This band is also the most intense observed in both IRMPD spectra and is also calculated to be the most intense in the calculated IR absorption spectrum of **MVal1**. The corresponding mode in **MVal2** has a calculated band intensity which is 39% of the most intense band of the spectrum at 1236 cm^{-1}. The experimental positions and intensities of this broad feature are in excellent agreement with the corresponding modes found for GlyMeH$^+$ and AlaMeH$^+$ with a slight decrease in frequency of each peak accompanying the increase in amino acid basicity as the alkyl group size increases.

On the basis of the calculated IR absorption bands of **MVal1** at 1258, 1303, and 1365 cm^{-1}, the IRMPD bands observed at 1243, 1287, and 1363 cm^{-1} can be assigned as bending and deformation modes of the ammonium, methyl, and isopropyl groups. An apparent discrepancy between experiment and theory appears in the relative intensity of the lowest energy maximum located at 1243 cm^{-1} (Figure 4a) where the experimental intensity is substantially higher than that calculated (0.79 vs 0.16). This might be because the two modes calculated to occur at 1258 and 1303 cm^{-1} correspond to normal modes displaying a large component on the bending motions of alkyl C−H groups. Their calculated relative intensities are therefore likely to be very sensitive to the method of calculation. This slight discrepancy associated to the relative intensities could also be due to the multiphoton nature of the IRMPD process as speculated previously by Kapota et al.[35] In essence, as the internal energy rises, the vibrational transitions are red-shifted and this red-shift might be of the order of magnitude of the energy difference between the two bands of interest (43 cm^{-1}). Nevertheless, the fact that a significant IRMPD rate is observed between 1300 and 1400 cm^{-1}, whereas the **MVal2** isomer does not present a significant IR absorption cross-section in this region, serves as an additional argument to exclude the existence of a significant population of this structure in our experimental conditions.

A broad feature is also observed in the 1000−1200 cm^{-1} region for ValMeH$^+$ with two maxima at 1054 and 1125 cm^{-1} assigned in the Paul trap. This is in good agreement with the low-energy part of the calculated spectrum of **MVal1** where bands are predicted to occur at 1084 and 1122 cm^{-1}. The calculated relative intensities are also similar to the experimental observation, again in contrast to those for **MVal2**.

5. Assignment of the IRMPD Spectrum of LeuMeH$^+$. The IRMPD spectra of LeuMeH$^+$ have been presented previously as a test case for comparison of spectra generated in a FTICR spectrometer relative to those obtained in a Paul-type ion trap.[54] For completeness, the important features of the LeuMeH$^+$ spectra are presented here as well as a more general discussion of FTICR vs Paul ion-trap IRMPD spectra below.

The IRMPD spectra of LeuMeH$^+$, reported in Figure 5a,b, exhibit a situation analogous to that observed for ValMeH$^+$ since the FTICR and ion trap spectra yield very similar frequencies

Table 1. Wavenumber Differences (in cm^{-1}) between Paul Ion-Trap Experiment and Calculation (Paul Trap−MAA1), FTICR and Paul Ion-Trap Experiments (ICR−Paul Trap), and Wavenumber Shifts (in cm^{-1}) Owing to the Two Possible $NH^+\cdots O$ Intramolecular Interactions (MAA1−MAA2) for the Protonated Amino Acid Esters of Glycine, Alanine, Valine, and Leucine

	$\delta\sigma$ -C═O stretch [1745–1771 cm^{-1} (cm^{-1})			$\delta\sigma$-NH_3 umb [1435–1471 cm^{-1}] (cm^{-1})			$\delta\sigma$-C–H bend [1247–1297 cm^{-1}] (cm^{-1})		
	Paul trap–MAA1	ICR–Paul trap	MAA1–MAA2	Paul trap–MAAI	ICR–Paul trap	MAA1–MAA2	Paul trap–MAA1	ICR–Paul trap	MAA1–MAA2
$GlyMeH^+$	+13	−26	−65	+32	−14	−59	+10	−25	+33
$AlaMeH^+$	+16	−19	−66	+18	−19	−44	+7	−21	+42
$ValMeH^+$	+4	−2	−64	−3	+16	−55	−11	−4	+22
$LeuMeH^+$	+5	−8	−63	+14	+1	−43	−4	−23	+33

of the band maxima with the ion-trap infrared spectrum showing slightly better resolution and a slight blue-shift relative to the FTICR infrared spectrum for certain bands. The two lowest energy structures **MLeu1** and **MLeu2** of the protonated monomer of $LeuMeH^+$ are also shown in Figure 5 together with their associated vibrational spectra given in spectra c and d, respectively. **MLeu1** is the lowest energy isomer while the **MLeu2** conformer lies 4.1 kcal mol^{-1} higher in energy.

Both the C═O stretch of the carbonyl group, and the NH_3^+ umbrella mode represent a clear-cut signature of the exclusive presence of the **MLeu1** structure in both experimental conditions. As discussed above in the case of glycine, alanine, and valine, these two normal modes are very sensitive to the hydrogen-bonding scheme in protonated monomer of $LeuMeH^+$. This bond is stronger for **MLeu1** than for **MLeu2** and, as a result, the NH_3^+ umbrella mode is red-shifted in **MLeu1** (1438 cm^{-1}) as compared to **MLeu2** (1481 cm^{-1}). The observed IRMPD band at 1452 cm^{-1} in the Paul trap spectrum is closer to the calculated position in **MLeu1**. The band observed at 1751 cm^{-1} in the Paul-trap spectrum is in very good agreement with the calculated position of the red-shifted carbonyl stretching mode for **MLeu1** of 1746 cm^{-1}.

As for the three other systems discussed above, a third structural diagnosis can be found in the 1200−1400 cm^{-1} energy range. Indeed, the Paul ion-trap infrared spectrum displays an IRMPD band at 1372 cm^{-1}, that is very close to the position of a calculated IR absorption band of **MLeu1** (1367 cm^{-1}), while no peak of any significant intensity is predicted in this region for **Mleu2**. This is again arguing for the dominant presence of **MLeu1**, the lowest energy isomer of protonated leucine methyl ester, under both experimental conditions. The higher intensity of the two bands is somewhat bimodal with local maxima at 1291 and 1305 cm^{-1} in the Paul ion-trap spectrum. The calculated spectrum of **MLeu1** predicts peaks at 1230, 1260, and 1295 cm^{-1}, whereas that for **MLeu2** predicts a single peak at 1232 cm^{-1} providing further support for the predominance of **MLeu1**.

Finally, the 800−1100 cm^{-1} energy range, only explored using the Paul trap, also provides an additional clear-cut infrared diagnostic in the present case. Indeed, the observed band at 875 cm^{-1} nicely matches the position (875 cm^{-1}) of the IR absorption associated with the NH_3^+ rocking mode of the **MLeu1** structure. On the contrary, no IRMPD signal was observed when scanning the photon energy around 1080 cm^{-1} which corresponds to the resonance of the NH_3^+ rocking mode of the **MLeu2** structure.

Discussion

1. IRMPD Spectra as a Diagnostic of Ion Structure. The present IRMPD results show that the 800−2000 cm^{-1} range of the infrared spectrum can be used to establish a conformational diagnosis of protonated amino acid derivatives. This work in particular shows that the comparison between experimental IRMPD spectra of mass-selected ions derived from methyl esters of amino acids and IR absorption spectra calculated by ab initio methods can provide a clear indication that the conformer found to be the most stable by calculations is that formed in greatest abundance under the experimental conditions of both MALDI ionization in a ICR cell and electrospray ionization in a Paul-type ion trap. The 1700−1850 cm^{-1} energy region is a clear-cut diagnostic for the presence of the most stable isomer, which exhibits a $C{=}O\cdots H^+$ intramolecular hydrogen-bonding interaction between the protonated amino group and the methoxy oxygen. Relative to the free carbonyl stretching frequency calculated for the second lowest energy conformer, characterized by a $C{-}(CH_3)O\cdots H^+$ intramolecular hydrogen bond, the CO stretching mode is systematically red-shifted by 64 ± 1 cm^{-1}. The red-shift of the NH_3^+ umbrella mode in the 1430−1500 cm^{-1} region also constitutes an infrared probe of the strength of the intramolecular hydrogen bond where the calculated red-shift is larger by 51 ± 8 cm^{-1} in the lowest energy isomer displaying the $C{=}O\cdots H^+$ intramolecular hydrogen bond. The agreement between the experimental and calculated positions of these bands is excellent. These results are summarized in Table 1. The position of the band corresponding to the C═O stretching mode differs by 4−16 cm^{-1} between that observed in the Paul ion-trap spectra and that calculated for MAA1. The location of the NH_3^+ umbrella mode in the spectrum recorded in the Paul trap differs by less than 18 cm^{-1} from the calculated value for MAA1, with the exception of the spectrum of $GlyMeH^+$ for which it is 32 cm^{-1}.

Using a similar experimental protocol, IRMPD spectroscopy has similarly been used to probe the protonation site of alanine dipeptide by Lucas et al.[37] These authors found that the recorded IRMPD spectrum was consistent with either of the two most stable conformations characterized by a $C{=}O\cdots H^+NH_2$ intramolecular hydrogen bond between the amide carbonyl group and the amino group. The carbonyl-stretch region provided a good structural diagnostic. Two peaks were observed at 1700 and 1760 cm^{-1} corresponding to the red-shifted amide carbonyl and to the free terminal carbonyl, respectively.

Similarly, the carbonyl stretch of glycine coordinated to a sodium cation has been shown by Kapota et al.[35] at CLIO to exhibit an absorption at 1727 cm^{-1} corresponding to a structure in which the sodium cation is "solvated" by the neutral glycine via both the carbonyl and amino groups. These studies are thus very encouraging and suggest that IRMPD spectroscopy can be a powerful technique for elucidating the conformational preferences in ionic species of biological interest in the gas

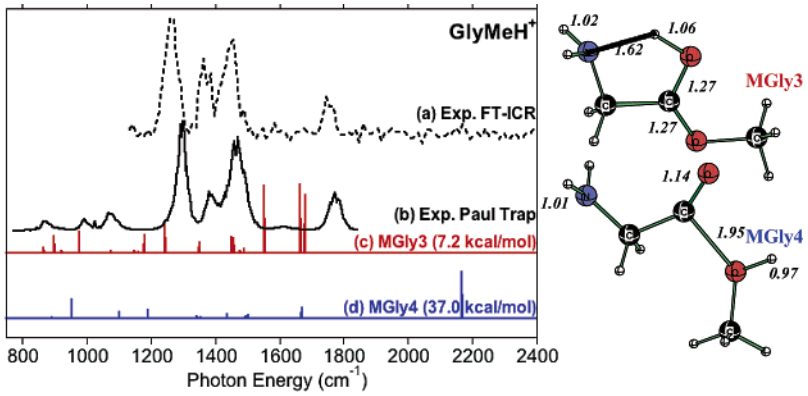

Figure 6. IR spectra of protonated glycine methyl ester $GlyMeH^+$: higher energy isomers. Experimental IRMPD spectrum recorded in the FTICR (a) and in the Paul ion trap (b) compared to the DFT calculated IR absorption spectra of energy conformers MGly3 (c) and MGly4 (d) located 7.2 and 37.0 kcal/mol above the ground state MGly1. The optimized structures of MGly3 and MGly4 are represented beside the spectra. The indicated distances are expressed in Å.

Table 2. Line Positions (in cm^{-1}) and (Relative Intensities) of the Main Maxima of the Experimental IRMPD Spectra Recorded in the Paul Ion Trap and Calculated IR Absorption Spectra Maxima for the Protonated Methyl Esters of Glycine, Alanine, Valine, and Leucine

	$GlyMeH^+$		$AlaMeH^+$		$ValMeH^+$		$LeuMeH^+$	
vib mode	IRMPD (Paul trap)	IR calcd (MGly1)	IRMPD (Paul trap)	IR calcd (MAla1)	IRMPD (Paul trap)	IR calcd (MVal1)	IRMPD (Paul trap)	IR calcd (MLeu1)
C−H bend	1297 (1)	1287 (0.66)	1286 (0.92)	1279 (0.54)	1247 (0.63)	1258 (0.16)	1291 (0.48)	1295 (0.30)
	1386 (0.32)	1372 (0.97)	1342 (0.40)	1357 (0.62)	1284 (0.79)	1303 (0.53)	1305 (0.64)	1295 (0.30)
							1372 (0.26)	1367 (0.54)
NH_3 umb	1471 (0.77)	1439 (0.61)	1456 (1)	1438 (1)	1435 (1)	1438 (1.0)	1452 (1)	1438 (1)
C═O stretch	1771 (0.35)	1758 (1)	1764 (0.24)	1748 (0.90)	1749 (0.26)	1745 (0.97)	1751 (0.63)	1746 (0.83)

phase. Furthermore, the systematic agreement between the experimental positions of the IRMPD bands and those calculated for the IR absorption of the lowest energy isomer shows that the most stable conformation is formed both in the MALDI process under FTICR conditions and in the electrospray process under Paul ion-trap conditions.

Finally, from the point of view of diagnostics, it is of interest to note the relative invariability of the frequencies of the three modes consistently observed to be the strongest in the experimental spectra, that is, the C−H bend, the NH_3 umbrella motion, and the C═O stretch. A comparison of the Paul ion-trap values observed for each of these modes, as well as those calculated for the most stable conformer, is summarized in Table 2. In the case of the C═O stretch there is a general slight decrease in the frequency of this mode with increasing size of the alkyl group which is accompanied by a similar but less pronounced change in the NH_3^+ umbrella-mode frequency. These two trends may indicate a slight increase in the intramolecular hydrogen-bond strength with increasing alkyl group size leading to a weakening of the carbonyl C═O bond and a corresponding decrease in frequency. Because of the increasing number and complexity of the C−H bending modes as the alkyl group size increases a clear trend is not evident in these modes; however, it does appear that a slight decrease in frequency also takes place.

2. Other Conformations of the Protonated Amino Acid Esters. In the results presented above only the isomers where protonation has taken place on the most basic site, i.e., the amino group, have been considered. Although these two isomers are calculated to be the most stable, the possible existence of other isomers in which protonation occurs at other basic sites has also been investigated.

Isomers of the protonated methyl ester of glycine, in which the proton is bound either to the oxygen of the carbonyl group or of the methoxy group, were shown to be local minima on the potential energy surface. The optimized geometries and the associated calculated IR spectra of two representative cases are reported in Figure 6, spectra c and d, respectively. In **MGly3**, which is calculated to lie 7.2 kcal mol^{-1} higher in energy than **MGly1**, the proton is bound to the oxygen of the carbonyl group but also interacts with the nitrogen lone pair of the amino group. This **MGly3** structure can be regarded as the result of a proton transfer from nitrogen to oxygen starting from the **MGly1** lowest energy structure. Conversely, if the proton is bound to the oxygen of the methoxy group, as in **MGly4**, the resulting structure is found to lie 37 kcal mol^{-1} higher in energy than **MGly1**. As is to be expected from the fact that these species are very high in energy, none of the characteristic features of these spectra can be found in the experimental IRMPD spectrum of $GlyMeH^+$. The principal IR signature of **MGly4** is an intense band at 2125 cm^{-1} corresponding primarily to the C═O stretch. All other bands located below 1700 cm^{-1} represent relative intensities lower than 20% of the maximum and might have been difficult to distinguish if they had been present, as noted above. In contrast, the IR spectrum of **MGly3** features very intense bands between 1000 and 1700 cm^{-1} with the most intense peak being located at 1632 cm^{-1}, corresponding to the symmetric deformation of the NH_2 group (NH_2 s-def). Very close in energy at 1645 cm^{-1}, the mode corresponding to a mixture of C═O stretch and NH_2 and OH bends, should also be prominent. The third very intense peak is located at 1522 cm^{-1} and corresponds to a mixture of C−C stretch and OH bends. The in-phase out-of-plane and in-plane bending modes of CH_2 (CH_2 wagging and scissoring) are respectively located

at 1324 and 1429 cm^{-1}, and the CH_3 symmetric deformation mode (umbrella) is at 1421 cm^{-1}. Finally, the vibrational mode corresponding to the in-plane OH bend occurs at 1256 cm^{-1}, and a combination of this mode with the in-plane CH_3 rocking mode should occur at 1156 cm^{-1}. Thus, in addition to the lack of correspondence to the C═O stretching mode, these additional features for **MGly4** and **MGly3** add further justification to rule out the presence of both isomers under either of the present experimental conditions.

3. Comparison of FTICR and Paul Ion-Trap IRMPD Spectra. The IRMPD spectra obtained using the two different experimental approaches display the same IRMPD features. Nevertheless, as noted above, the dominant IRMPD bands observed using the FTICR are slightly red-shifted relative to the analogous bands in the Paul-trap spectra. This systematic shift is illustrated by the comparisons outlined in Table 1 for the key structurally diagnostic vibrational modes in the spectra. In general, it can be seen that as the size of the alkyl group increases for this set of four amino acid esters, the difference between the positions observed in the FTICR and Paul ion-trap spectra diminishes. The resolution of the IRMPD spectroscopy is also affected by the experimental conditions. While the full width at half-maximum (fwhm) of the bands of the IRMPD spectra recorded using the FTICR are of the order of 40 cm^{-1}, a better resolution (20 cm^{-1}) is obtained using the Paul trap. This relatively consistent behavior then leads to some speculation concerning the reason or reasons leading to these observations. In this context, it is useful to analyze the differences between the experimental conditions for the two sets of spectra.

The overlap between the ion cloud and the infrared beam is a critical parameter. It is generally believed that the ion confinement in a Paul ion-trap device is further enhanced by the collisions with helium buffer gas. On the other hand, the ensemble of ions trapped in the FTICR executes relatively complex motions resulting from the combination of the cyclotron motion with two large amplitude motions. As noted in the Experimental Methods section, the mass-selected molecular ions trapped in the ICR cell were irradiated for 1 s, which constitutes 25 macropulses, while a single FEL macropulse was used under Paul ion-trap conditions. Considering that the resulting fragmentation efficiencies are of the same order of magnitude, this suggests that the overlap between the ion cloud and the infrared beam is more efficient in the Paul trap than in the ICR cell where the two large amplitude motions of the ions limit their overlap with the infrared beam. Using a single FEL macropulse, 100% fragmentation yield can be observed using the Paul ion trap, which clearly shows that the multiple photon absorption process inducing the fragmentation of the ions may occur within a single macropulse in the Paul trap. Under FTICR conditions, the overlap between the laser beam and the ion cloud is limited by the large amplitude motions of the ions. As a result, optimizing the fragmentation yield by tuning the focalization of the infrared beam in the ICR cell is the result of a compromise. The optimized beam waist at the center of the ICR cell was measured to be ~1.5 mm at 1000 cm^{-1} and ~0.7 mm at 2000 cm^{-1}, thus significantly smaller than the estimated size of the ion cloud which is controlled by two large amplitude motions. First, the relatively slow, typically with a ms period, and large amplitude (~3 to 4 mm) magnetron motion about the magnetic axis limits the number of ions that can be irradiated by a single 8 μs long macropulse. Allowing for a longer irradiation time, virtually all ions will transect the infrared beam. Second, large amplitude (~3 to 4 mm) oscillations of the ions along the magnetic axis, due to the motion in the field created by the trapping voltages, limit the overlap of a given ion with a macropulse since the period of these oscillations is typically of the order of μs. As a result, multiple photon absorption may occur but will not necessary induce fragmentation for all of the irradiated ions. It is thus conceivable that, for a fraction of the ions, the number of absorbed photons within a macropulse might not be sufficient to induce the fragmentation.

The combined effects of this potentially slow heating by the FEL and the absence of collisional cooling owing to the low pressures in the FTICR cell could be at the origin of the red-shift of the bands observed under FTICR conditions. Indeed, as the irradiation time increases, the internal energy of an increasing fraction of the ion population will be raised, but not sufficiently to dissociate. As a function of the irradiation time, the internal energy distribution of the ion cloud would thus increase, and the net result would be a red-shift of the infrared cross-section associated with the vibrational mode in the 1000−2000 cm^{-1} energy range, because of the cross-anharmonicity couplings with the vibrationally excited low-energy modes. This red-shift of the infrared cross-section associated with the multiple photon absorption process has been used to rationalize the red-shift of the IRMPD bands as compared to the calculated linear absorption spectrum.

In contrast, ions in the Paul trap are continuously collisionally cooled by the high pressure of He present in the trap. One could thus expect a Boltzmann distribution of the internal energy of the ions prior to their irradiation by a macropulse, with a temperature of the ion in a Paul trap of the order of 310 ± 20 K, as estimated by Gronert.[68] This should then result in a narrower peak with a maximum at a photon energy close to the calculated maximum of the 0 K cross-section. This is, in essence, what is observed in the present case where the Paul ion-trap peaks are both narrower and at higher energy that those in the FTICR spectra. As noted above however, as the molecular size increases the differences between FTICR and Paul ion-trap spectra become smaller. This can be rationalized on statistical grounds. For a given amount of internal energy and/or given heating rate for two populations of ions with differing numbers of normal modes, there is a lower probability that the larger species will have modes other than $v = 0$ populated. Thus less of a red-shift would be anticipated for the ions in the FTICR experiment and the peaks would be more nearly comparable in width. Once again, this is what is observed experimentally. On this basis, it is likely that the Paul ion-trap spectra more closely resemble the true thermal situation.

4. Fragmentation Pathways. Understanding the dissociation chemistry of protonated peptides, whether induced via photo absorption, collisional activation, or electron capture, has become a vigorous research area as a result of the growing mass-spectrometric activity associated with proteomics.[69] The "mobile proton" model assumes that, upon activation, the excess proton may migrate from one basic site to another such that the system samples many different local minima on the potential energy surface. As a result many different fragmentations, resulting

(68) Gronert, S. *J. Am. Soc. Mass Spectrom.* **1998**, *9*, 845.
(69) Paizs, B.; Suhai, S. *Mass Spectrom. Rev.* **2005**, *24*, 508.

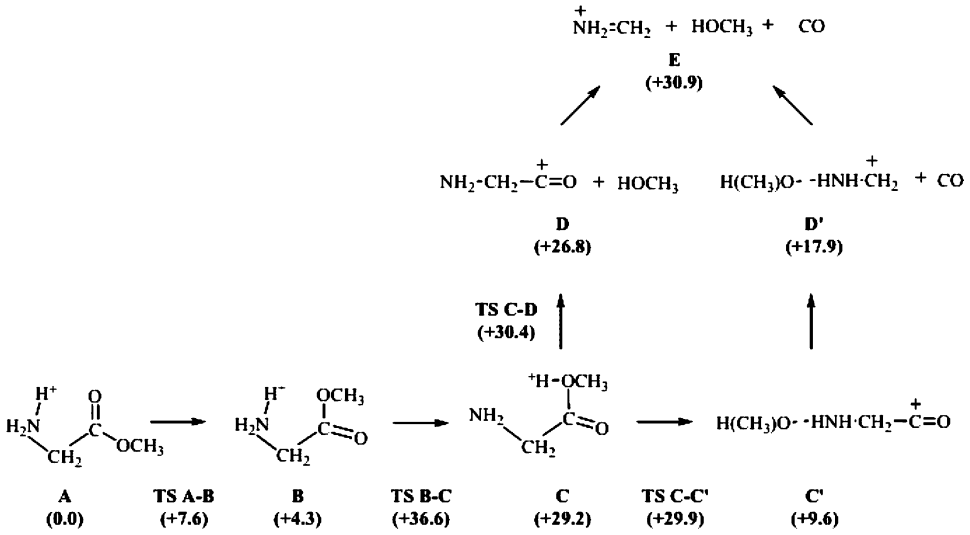

Figure 7. Suggested mechanisms for the photofragmentation of the methyl ester of glycine. The intermediates of the two pathways leading to sequential loss of carbon monoxyde and methanol are represented. The numbers in parenthesis are the relative enthalpies at 0 K of the corresponding intermediates for the fragmentation of protonated glycine, with respect to its most stable isomer, calculated by Rogalewicz and Hoppiliard at the MP2 level of theory.[64] The values are expressed in kcal/mol.

from these minima, may occur in a structurally revealing way. However, this model is generally limited to qualitative interpretations, and a deeper understanding of the relationships between conformation and fragmentation patterns is definitely warranted.[69] The IRMPD fragments observed in the present work can provide some insight into these dissociation dynamics and pathways.

As noted above, the IRMPD spectra have been obtained by monitoring the appearance of the immonium cation fragment ions, $(R)CH{=}NH_2^+$. Such ions were also found to be the major fragment ions resulting from CID of α-amino acid methyl esters[70] and are commonly observed as major fragment ions resulting from CID experiments on amino acids without functional groups[65,71] and small peptides.[71] Under low-energy CID conditions, peptide fragmentation has also been found to lead to a minor acylium fragment ion, the so-called b ion,[72,73] which is associated with the loss of H_2O from the protonated peptide. In the case of protonated glycine, a theoretical study of the fragmentation pathways[64] has suggested that under low-energy CID, fragmentation occurs through a consecutive loss of H_2O leading to an acylium ion, which in turn spontaneously loses CO leading to an immonium ion. It should be noted that, in the present case, acylium fragments were not observed under IRMPD conditions and that the $(CH_3)CH{=}NH_2^+$ immonium ion was also the only fragment observed for IRMPD of protonated dialanine using the same MALDI/FTICR experimental protocol.[37]

In the case of the methyl esters of amino acids studied in the present work, this fragment corresponds to a loss of 60 *m/z* units, that is, [2C,2O,4H]. By analogy to protonated glycine,[64] this composition could correspond to (i) methyl formate, ($HCOOCH_3$); (ii) carbon dioxide and methane ($CO_2 + CH_4$); (iii) methoxy−hydroxy carbene ($:C(OH)(OCH_3)$); or (iv) methanol and carbon monoxide ($CH_3OH + CO$). A detailed ab initio study of the potential-energy surface for the fragmentation of protonated glycine, leading to the analogous four products, has been carried out by Rogalewicz and Hoppiliard,[64] which confirms that the lowest energy pathway is the sequential loss of CO and H_2O, in agreement with the commonly presumed mechanism suggested by low-energy CID experiments.[65] In the case of IRMPD experiments, the energy of the system increases by sequential absorption of several isoenergetic low-energy photons. Therefore it is to be expected that the major fragmentation pathway will be that with the lowest energy threshold, as long as absorption is allowed. By analogy to the results of Rogalewicz and Hoppiliard,[64] this should correspond to the formation of methanol and carbon monoxide for the protonated methyl esters of the amino acids studied here. The two possible pathways leading to these products suggested by Rogalewicz and Hoppiliard[64] adapted to the methyl ester of glycine, are shown schematically in Figure 7.

The rate-limiting step for the sequential loss of CO and CH_3OH would thus be expected to be proton migration from the nitrogen to the oxygen of the ester function (**TS B−C**) which would require 36.6 kcal mol^{-1}, corresponding roughly to the absorption of 13 photons at 1000 cm^{-1}. This is entirely feasible given the magnitude of laser powers used in this study. The first intermediate on the pathway for the ultimate formation of the immonium ion **E** via loss of CO and CH_3OH is isomer **B**, which requires a rotation about the C−C bond from the most stable structure **A**. This step is endothermic by only 7.6 kcal mol^{-1} for the analogous system examined by Rogalewicz and Hoppiliard.[64] Intermediate **C** results from the endothermic intramolecular proton transfer from **B**, and from **C** two possible pathways can be considered. The first of these involves direct loss of methanol leading to the acylium ion **D**, 26.8 kcal mol^{-1} higher in energy than **A**, while the second proceeds via formation of another stable intermediate **C′**, located 9.6 kcal mol^{-1} higher in energy than **A**. Somewhat surprisingly, **C′** is more energetically favorable than **C**, presumably as a result of

(70) Bouchoux, G.; Bourcier, S.; Hoppiliard, Y.; Mauriac, C. *Org. Mass Spectrom.* **1993**, *28*, 1064.
(71) Klassen, J. S.; Kebarle, P. *J. Am. Chem. Soc.* **1997**, *119*, 6552.
(72) Poppe-Schriemer, N.; Ens, W.; O'Neil, J. D.; Spicer, V.; Standing, K. G.; Westmore, J. B.; Yee, A. A. *Int. J. Mass Spectrom. Ion. Proc.* **1995**, *143*, 63.
(73) Yalcin, T.; Khoum, C.; Csizmadia, I. G.; Peterson, M. R.; Harrison, A. G. *J. Am. Soc. Mass Spectrom.* **1995**, *6*, 1164.

stabilization by the intermolecular hydrogen bond in this ion-neutral complex. Elimination of carbon monoxide from **C′** would lead to **D′** via a barrierless bond cleavage. Loss of CH_3OH from **D** or CO from **D′** would lead to the immonium ion **E**, 30.9 kcal mol^{-1} higher in energy than **A**. Interestingly, it has been previously shown that protonation of the methyl esters of carboxylic acids leads to substantial elimination of CH_3OH to form stable acylium ions,[74−77] which would be in agreement with the mechanism involving **D** suggested here.

Conclusion

This work illustrates the significant conformational insight which may be derived from gas-phase mid-infrared spectroscopy of protonated compounds of biological interest. The synergism between gas phase infrared spectroscopy experiments and ab initio calculations is critical. We show that the most stable conformations of the four simplest protonated methyl esters of amino acids, $GlyMeH^+$, $AlaMeH^+$, $ValMeH^+$, and $LeuMeH^+$, when formed either by MALDI in the ICR cell or by ESI in a Paul ion trap, preferentially adopt the most stable conformation predicted by ab initio calculations. This structure presents an intramolecular interaction between the protonated amino group and the carbonyl function. The agreement between the IRMPD spectra and the calculated IR spectra of the most stable conformers is very good in all cases. The IR spectra of the four amino acid esters present common features providing evidence for the intramolecular interaction between the protonated amino group and the carbonyl function which is characteristic of the most stable structure. A comparison of the IR absorption spectra of the two most stable calculated conformers reveals a systematic red-shift of -64 ± 1 cm^{-1} for the carbonyl stretch and of -51 ± 8 cm^{-1} for the NH_3 umbrella mode when the carbonyl group is involved in the hydrogen bond. A similar study is currently being performed for the proton-bound dimers of the methyl esters of the amino acids studied here and will be presented in a future contribution.

Acknowledgment. The generous financial support of the Natural Sciences and Engineering Research Council of Canada is gratefully acknowledged. The financial support of the European Commission through the NEST/ADVENTURE program (EPITOPES, Project No. 15637) is also gratefully acknowledged. This work was also supported by the CNRS and the laser center POLA at the Université Paris-Sud 11. We thank François Glotin, Jean-Michel Ortega, and the technical staff at the CLIO facility for their support during the experiments. We also thank Gérard Mauclaire, Michel Héninger, Gérard Bellec, and Pierre Boissel who, together with one of us (J.L.), provided us with the mobile FT-ICR mass spectrometer used in this work.

Supporting Information Available: Complete ref 55; SI Tables 3−6 showing positions and intensities of the bands observed in the IRMPD spectra and calculated IR spectra for the two lowest energy conformers of $GlyMeH^+$ (Table 3), $AlaMeH^+$ (Table 4), $ValMeH^+$ (Table 5), and $LeuMeH^+$ (Table 6); a description of the nature of the most intense vibrational modes. This material is available free of charge via the Internet at http://pubs.acs.org.

JA0662321

(74) Harrison, A. G.; Kallury, R. K. M. R. *Org. Mass Spectrom.* **1980**, *15*, 277.
(75) Tsang, C. W.; Harrison, A. G. *J. Chem. Soc., Perkins Trans. 2* 1975, 1718.
(76) Weinkam, R. J. *J. Am. Chem. Soc.* **1974**, *96*, 1032.
(77) Weinkam, R. J.; Gal, J. *Org. Mass Spectrom.* **1976**, *11*, 188.